JARO 15: 305–317 (2014)
DOI: 10.1007/s10162-013-0438-4

JARO
Journal of the Association for Research in Otolaryngology

Research Article

Human Yaw Rotation Aftereffects with Brief Duration Rotations Are Inconsistent with Velocity Storage

Andrew J. Coniglio[1] and Benjamin T. Crane[2,3,4]

[1]*School of Medicine, University of Rochester, 601 Elmwood Avenue, Box 260, Rochester, NY 14642, USA*

[2]*Department of Otolaryngology, University of Rochester, 601 Elmwood Avenue, Box 629, Rochester, NY 14642, USA*

[3]*Department of Neurobiology and Anatomy, University of Rochester, 601 Elmwood Avenue, Box 629, Rochester, NY 14642, USA*

[4]*Department of Bioengineering, University of Rochester, 601 Elmwood Avenue, Box 629, Rochester, NY 14642, USA*

Received: 13 September 2013; Accepted: 20 December 2013; Online publication: 10 January 2014

ABSTRACT

In many sensory systems, perception of stimuli is influenced by previous stimulus exposure such that subsequent stimuli may be perceived as more neutral. This phenomenon is known as an aftereffect and has been studied for vision, audition, and some vestibular stimuli including roll and translation. Previous data on yaw rotation perception has focused on low-frequency stimuli on the order of a minute which may not be directly applicable to frequencies during ambulation. The aim of the current study is to look at the influence of yaw rotation on subsequent perception near 1 Hz, the predominant frequency of yaw rotation during human ambulation. Humans were rotated with 12 ° whole body adapting stimulus over 1 or 1.5 s. After an interstimulus interval (ISI) of 0.5, 1.0, 1.5, or 3 s, a test stimulus the same duration as the adapting stimulus was presented, and subjects pushed a button to identify the direction of the test stimulus as right or left. The direction and magnitude of the test stimulus was adjusted based on prior responses to find the stimulus at which no rotation was perceived. Experiments were conducted both in darkness and with a visual fixation point. The presence of a fixation point did not influence the aftereffect which was largest at 0.5 s with an average size of 0.78±0.18 °/s (mean±SE). The aftereffect diminished with a time constant of ~1 s. Thresholds were elevated after the adapting stimulus and also decreased with a time constant of ~1 s. These findings demonstrate that short adapting stimuli can induce significant aftereffects in yaw rotation perception and that these aftereffects are independent from the previously described velocity storage.

Keywords: post-roll illusion, aftereffects, motion aftereffect, velocity storage, vestibular, semi-circular canal, rotation

INTRODUCTION

The vestibular system drives reflexes and also drives perception including orientation. The challenges to the vestibular system are different in these roles, and thus, vestibular reflexes often do not correlate with perception (Barnett-Cowan et al. 2005; Merfeld et al. 2005a; Bertolini et al. 2011). For instance the vestibulo-ocular reflex (VOR) must respond similarly to every head movement for visual stability to be maintained, while it is much less important for perception of repetitive movements be the same each time the stimulus is encountered.

A further challenge the vestibular system faces is that the semicircular canals do not directly encode head velocity but rather they detect the motion of fluid in the canals relative to the surrounding bone. Therefore, a continuous rotation cannot be encoded because the fluid will reach the velocity of the surrounding bone with a time constant of ~4 s (Goldberg and Fernandez 1971; Dai et al. 1999; Ifediba et al. 2007). A central velocity storage mech-

Correspondence to: Benjamin T. Crane • Department of Otolaryngology • University of Rochester • 601 Elmwood Avenue, Box 629, Rochester, NY 14642, USA. Telephone: +1-585-7585700; fax: +1-585-271-8552; email: craneb@gmail.com

anism (VSM) acts to prolong this signal to a time constant of 10–30 s (Young and Oman 1969; Cohen et al. 1981; Bertolini et al. 2011), thus correcting for this deficiency of the semicircular canal and providing a better estimate of head motion (Laurens and Angelaki 2011). This VSM is most frequently studied during velocity steps or after such rotations have abruptly stopped (Cohen et al. 1981; Keller and Henn 1984; Okada et al. 1999; Sinha et al. 2008; Bertolini et al. 2011; Bertolini et al. 2012). Thus the influence of the VSM on perception of low-frequency stimulation is clear, in that it causes the perception to persist with a time constant consistent with the VSM.

The potential influence of the canal physiology and the VSM has also previously been considered for perception of isolated yaw rotations of shorter durations. It has been shown that the threshold of yaw rotation perception sharply increases below frequencies of about 0.2 Hz (Benson and Brown 1989; Grabherr et al. 2008; Soyka et al. 2012). Modeling of these velocity thresholds has shown that this increase occurs at higher frequency than would be predicted by models of VSM or even the time constant of the semicircular canal itself (Grabherr et al. 2008).

The current paper investigates the possibility that the VSM might influence perception of recurring yaw rotations above 0.5 Hz. This is a highly relevant frequency realm because prevalent frequency of yaw rotation during human ambulation is near 1 Hz (Grossman et al. 1989; Crane and Demer 1997). In many areas of sensory perception, exposure to a stimulus causes a subsequent similar stimulus to be perceived as more neutral. Similarly, presentation of a neutral stimulus may be perceived as opposite the initial stimulus. A classic example is the "waterfall illusion," a visual motion aftereffect in which shifting gaze from a waterfall to nearby rocks causes the perception that they are moving upward (Addams 1834). Such aftereffect phenomena have been described over a wide range of frequencies in vision (Anstis et al. 1998; Thompson and Burr 2009), audition (Reinhardt-Rutland 1990; Bestelmeyer et al. 2010), and proprioception (Seizova-Cajic et al. 2007). Vestibular aftereffects have been described with fore-aft translation (Crane 2012b) and roll (Ercoline et al. 2000; Nooij and Groen 2011; Crane 2012a). These aftereffects occur via multiple neural mechanisms (Mather et al. 2008). The goal of the current study is to examine the influence of prior yaw rotation on perception of subsequent vestibular stimuli.

MATERIALS AND METHODS

Equipment

Motion stimuli were delivered using a 6-degree-of-freedom motion platform (Moog, East Aurora, NY, USA, model 6DOF2000E) similar to that used in other laboratories for human and monkey motion perception studies (Grabherr et al. 2008; Fetsch et al. 2009; MacNeilage et al. 2010; Valko et al. 2012) and previously used for translation (Crane 2012b) and roll (Crane 2012a) aftereffect studies in the current laboratory. Subjects were seated upright in a padded racing seat (Corbeau, Sandy, UT, USA, model FX-1) mounted on the platform which included high lumbar and seat bolsters. The head was fixed using an appropriately sized football style helmet which was rigidly fixed to the motion platform with an inflatable liner to prevent decoupling of the head as previously described (Crane 2012b).

In some trials, a visual fixation point was presented on a horizontal color LCD screen measuring 115.6 by 64.8 cm with a resolution of 1,920×1,080 pixels (Samsung model LN52B75OU1FXZA). The subject was seated 50 cm from the screen that filled a 98 ° field of view in azimuth. A fixation point consisted of a 2×2 cm midline cross at eye level.

A masking noise was delivered as previously described (Roditi and Crane 2012b). The rotation axis was adjusted so it was always located between the external auditory canals to minimize lateral translation of the labyrinth.

A hand-held button box was used to collect responses. The center button was pressed by the subject to initiate each stimulus. The two buttons at either end were used to identify the perceived direction of yaw rotation as left or right.

Stimuli

All trials included a test stimulus in which the subject was asked to report the perceived direction of rotation. Aside from a control condition in which only the test stimulus was presented, in most trial blocks, there was also included an adapting stimulus which when present always preceded the test stimulus (Fig. 1). There was an interstimulus interval (ISI) in which no motion occurred between the adapting and test stimuli. The adapting stimulus was always a constant amplitude of 12 °, but for each block of trials, the direction was randomly interleaved such that it could occur in either the right or left direction. Following the randomized adapting stimulus, the test stimulus could also be in either the rightward or leftward direction. Unlike the adapting stimulus, however, the amplitude and direction of test stimulus was adjusted based on a subject's prior responses. Both stimuli consisted of a sine wave in acceleration, 1 s in duration for most experiments. The equations which describe these stimuli have been previously published (Crane 2012b) and are similar to those used in other motion perception studies (Benson et

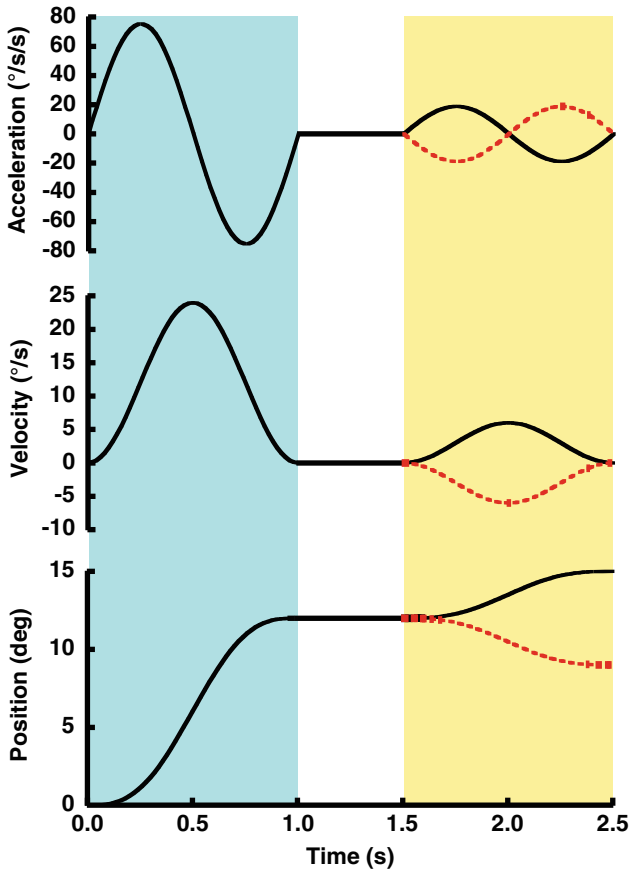

FIG. 1. Diagram of the motion experienced by a subject during example trials with a 1 s adapting stimulus, 0.5 s ISI, and 1 s test stimulus. The examples shown would have occurred at the start of a trial block when the largest test stimuli (3 °) were used. In this example, the adapting stimulus was 12 ° of motion to the right and is the same for both trials. The same movement is shown in the acceleration (*top panel*), velocity (*middle panel*), and position (*bottom panel*) domains. The adapting stimulus occurred during the initial 1 s (*blue shading*), the ISI from 1 to 1.5 s (*no shading*), and the test stimulus from 1.5 to 2.5 s (*yellow shading*). The test stimulus could be in either direction: right (*black*) and left (*red dashed*).

al. 1986; Grabherr et al. 2008; Crane 2012a). A small amount of mechanical oscillation limited to the fore-aft direction was added to each test stimulus presentation to minimize non-vestibular cues such as noise and vibration (Crane 2012b).

The experiment was performed in two ways: with a visual fixation point (FP) and with no fixation (NF) point. The FP was a 1-cm cross on a video display centered between the eyes at eye level. The rest of the screen was dark. Partitions on the sides and top of the screen obstructed from view any earth-fixed objects which could have given cues to the direction of movement. The NF trials were conducted in darkness. During both sets of trials, the right eye position was monitored and recorded at 60 Hz using an infrared video eye tracking system (LiveTrack, Cambridge Research Systems, Rochester England). The eye tracking system was predominantly used to ensure subjects maintained fixation during the FP trials even though lack of distracting stimuli made fixation failures extremely rare.

Trial blocks included trials with a single viewing condition (FP or NF) and ISI. In two blocks of trials (one FP and one NF), only the test stimulus and no adapting stimulus was given. In the remaining eight trial blocks, each test stimulus was preceded by an adapting stimulus. Each of these trial blocks included a single ISI of 0.5, 1.0, 1.5, or 3.0 s and was done with a FP and with NF. The order in which trial blocks were completed was randomized for each subject. After each test stimulus, the subject returned to the starting position. The adapting stimulus was always 12 ° (peak velocity 24 °/s, peak acceleration 75 °/s/s) with leftward and rightward adapters randomly interleaved so that adapters of both directions were evenly distributed and unpredictable within a trial block.

The maximum test stimulus amplitude was 3 ° over 1 s (1.0 Hz, peak velocity 6 °/s, peak acceleration 19 °/s/s). An adaptive staircase was used to determine which stimuli to present next based on previous responses. The staircases were designed to start with stimuli large enough to be unambiguously perceived and work toward smaller stimuli. Interleaved independent staircases were used, one staircase started with rightward rotation and the other with leftward rotation. This was done to eliminate any potential artifacts based on the initial test stimulus and minimize the ability of subjects to identify patterns in the stimulus presentation. Each pair of staircases contained 50 stimulus presentations; thus, each block of trials using an adapting stimulus included 100 pairs of adapting and test stimuli. After each response the stimulus velocity was adjusted in the opposite direction. Thus, the staircases tended to deliver most stimuli in a range where subjects were likely to perceive a movement in either direction equally. However, there were not necessarily equal numbers of test stimuli on either side of zero. With each reversal in response direction, the step size decreased by half down to a minimum of 0.4 °/s. The level was changed in a 1-up, 1-down manner—i.e., a leftward response causes the next stimulus to be delivered in a more rightward direction and vice versa. If the subject did not respond with a perceived direction within 2 s, no response was recorded, and the stimulus was re-presented when that staircase was active again. These types of lapses were rare and occurred in <1 % of stimulus presentations. This type of algorithm has been previously used in the current laboratory (Crane 2012b, a; Roditi and Crane 2012a; Crane 2013) as well as by others (Fetsch et al. 2009; MacNeilage et al. 2010).

An additional test condition was performed about 1 year after the initial experiments. This test consisted of a 1.5 s, 12 ° adapting stimulus (0.66 Hz, peak velocity 16 °/s, peak acceleration 33.5 °/s/s) and a 1.5 s test stimulus. The ISIs tested (0.5, 1.0, 1.5, and 3 s) were similar to the previous condition, and all trials were collected with NF point.

Subjects

A total of nine human subjects participated in the experiment. There were three women and six men with a mean age of 46±18 (mean±SD, range 20–69). Subjects were chosen to cover the range of ages in the adult population. Prior studies have not shown thresholds of rotation perception to vary by age in this range (Roditi and Crane 2012b). To prevent fatigue, trial blocks were completed over three to five testing sessions which took place on separate days. Subjects took breaks between trial blocks on the same day. Informed written consent was obtained from all participants. Two of the subjects (4 and 7) were familiar with the design of the experiment, and the remaining subjects were naïve. The protocol was approved by the University of Rochester Research Science Review Board.

All subjects were screened prior to participation. The screening included caloric testing, an audiogram, visual acuity testing, and screening questions to rule out any known history of vestibular disease or cognitive deficit. Based on these results, the subjects had normal peripheral vestibular function and hearing.

Analysis

The percentage of rightward responses for each stimulus level was plotted as a function of the test stimulus delivered (Fig. 2). A cumulative Gaussian function with confidence intervals was determined from those data points using a Monte Carlo maximum-likelihood criteria as previously described (Wichmann and Hill 2001a, b) and used by others (Fetsch et al. 2009; MacNeilage et al. 2010) as well as in the current laboratory (Crane 2012b, a; Roditi and Crane 2012a). Data from each subject was resampled and fit 2,000 times so that multiple estimates of the mean and standard deviation could be generated and 95 % confidence intervals determined based on the upper and lower bounds that contained 95 % of the estimates (Fig. 3(C)). The mean of the psychometric function is referred to as the bias. Thus, if the mean is at zero (common when no adapting stimulus was present), there is no bias. Very frequently, the psychometric function was shifted such that a neutral stimulus would be perceived in the direction opposite the earlier adapting stimulus. This type of bias is referred to as an aftereffect. The term aftereffect relates the direction of the bias to the direction of the adapting stimulus. The size of the aftereffect was determined by subtracting the bias with a rightward adapting stimulus from the bias with a leftward adapting stimulus and dividing

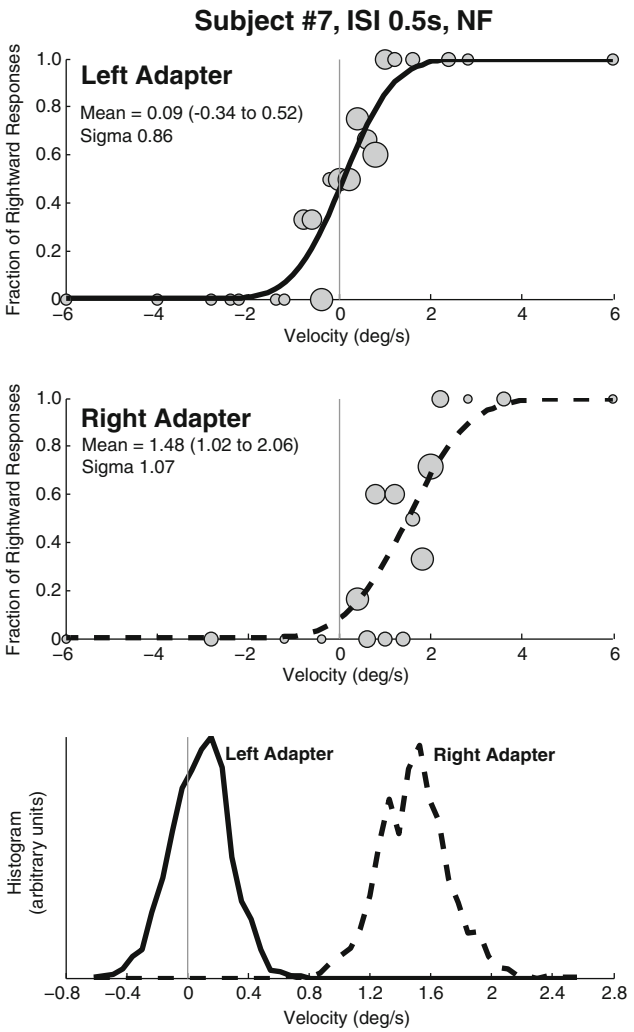

FIG. 2. Example data from a block of trials of a typical subject (#7) with an ISI of 0.5 s and a 1 s adapting/test stimulus. *Gray circles* in the two upper panels are sized proportionally to the number of responses represented. A CDF was calculated from each data set as a method of determining the mean (bias) and sigma (threshold) for each test condition. In this subject, the shift in the CDF was larger with the rightward adapter. Although such asymmetries were common, they did not occur systematically in the same direction. *Top panel*: Best fit of a CDF to trials in which the adapting stimulus was to the left. The mean of the CDF is near zero. *Middle panel*: The CDF fit to trials in which the adapting stimulus was a rightward rotation. The mean is shifted towards right indicating that a neutral stimulus is now more likely to be perceived as left. *Bottom panel*: The CDF was fit to the data in the previous panels after being randomly resampled 2,000×. The histograms of these fits are shown which demonstrates a significant difference between the two curves with no overlap. The *y*-axis is of arbitrary units and is not labeled.

by two in each of the 2,000 fits thus allowing a mean and 95 % confidence interval to be determined. This curve fitting method was also applied to data combined across subjects so that parameters could be determined. In every case, the aftereffect found by averaging the individual fits was within 0.1 °/s of that obtained by fitting combined data.

The repeated measures analysis of variance (ANOVA) was used to compare the bias between subjects and test conditions for conditions when an adapting stimulus was given. Factors included adapter direction and ISI. The Kruskal–Wallis test was also performed as a non-parametric test when an ANOVA was found to be significant. Pearson's correlation coefficient was used to test the significance of correlations between groups. Statistical significance was defined as $p<0.05$.

The parameters of an exponential decay function were fit to individual aftereffect responses using the equation, $y=Ce^{-t/\tau}$, where y is the size of the aftereffect, C is a constant, and τ is the time constant. This was done using the solver function in Microsoft Excel with the objective of minimizing the error between the predicted and observed aftereffect size.

A control systems model of vestibular perception was implemented (MATLAB Simulink module—version 2012b) which incorporated the major features of the models previously developed for velocity storage in eye movement recording (Robinson 1977; Raphan et al. 1979), then modified for use with vestibular perception with velocity (Bertolini et al. 2011), and recent models of yaw perceptual thresholds (Grabherr et al. 2008; Soyka et al. 2012).

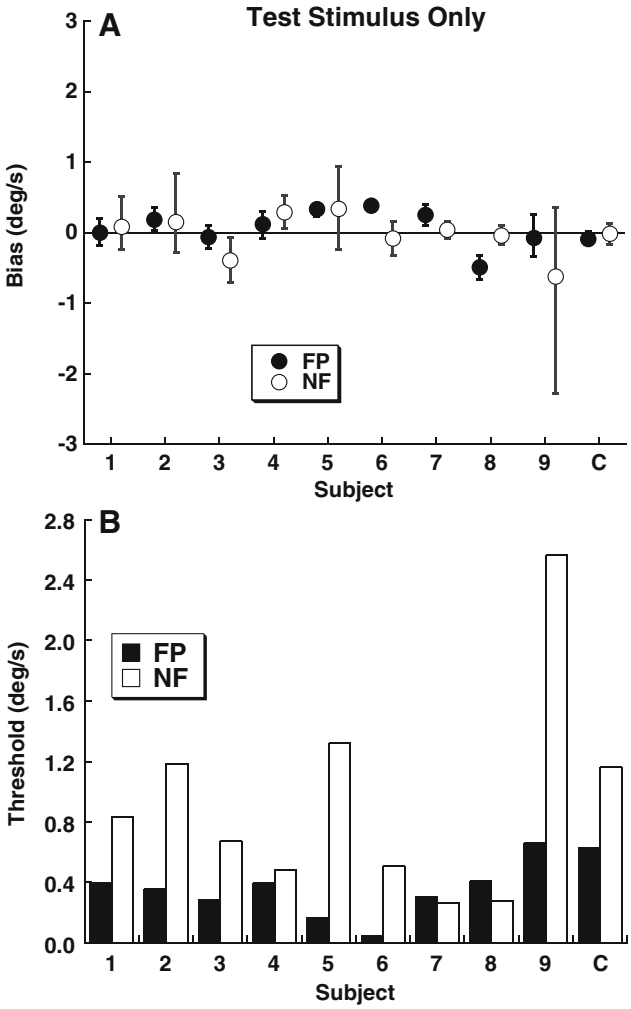

FIG. 3. Bias (mean of CDF) and threshold (sigma of CDF) for the test stimulus without an adapting stimulus by subject. The final column represents the CDF fit from all the responses combined across subjects (*C*). Filled symptoms represent a visible FP, and open symptoms represent trials done in darkness with NF. **A** Bias of the psychometric function with error bars representing the 95 % confidence interval. **B** Thresholds for the FP and NF conditions.

RESULTS

All subjects were able to correctly and reliably identify direction of the test stimulus at the extreme range: 3 ° of motion (peak velocity 6 °/s) presented after the larger adapting stimulus at the beginning of the staircase.

The baseline bias (mean of the cumulative distribution function (CDF)) and threshold (sigma of the CDF) was determined by fitting a CDF to each subject's responses (Fig. 2) using the test stimulus without an adapting stimulus. In every instance the bias was <0.6 °/s (Fig. 3A). For a 1 s test stimulus, mean bias had a peak velocity of 0.22± 0.18 °/s. The bias was similar between the FP and NF conditions (ANOVA, $p=0.94$, $F=0.006$). The threshold was lower in seven of the nine subjects in the FP condition when compared with NF (Fig. 3B). With the FP, the mean threshold was 0.33±0.17 °/s (mean±SD), while in the NF point condition, it was 0.90±0.72 °/s. The higher threshold in the NF condition relative to FP was not statistically significant (ANOVA, $p=0.04$, $F=5.19$; Kruskall–Wallis, $p=0.17$).

A 1 s long, 24 °/s peak velocity adapting stimulus given prior to a 1 s test stimulus influenced how the test stimulus was perceived. The overall perception of the test stimulus was biased in the opposite direction of the adapting stimulus (Fig. 4) such that the bias represented an aftereffect. Similar to the test stimulus-only condition, the presence or absence of a visual reference point (FP vs. NF) had no significant influence on the bias (ANOVA, $p=0.88$, $F=0.024$). The significance of the adapter's influence on the bias was determined by performing multiple samplings and a refitting of the subjects' data as described in the

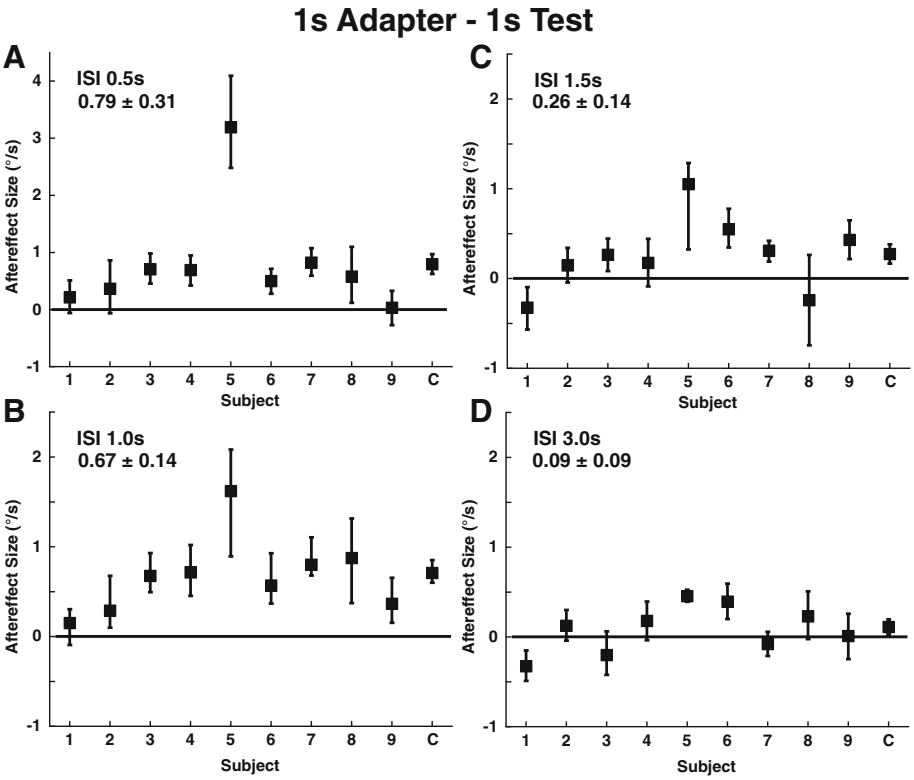

FIG. 4. Size of aftereffect by subject using a 1 s adapter and 1 s test stimulus. Each data point represents the median aftereffect size calculated using a bootstrapping method with 2,000 fits to the data after resampling. Trials with NF and FP were combined as these conditions had no influence on the bias. The mean±SE of the individual responses is shown in the *upper left* of each panel. The scale of the *y*-axis in **(A)** has been expanded relative to the others to allow an outlying data point to be shown. Error bars represent the 95 % confidence interval. Panel **A**: ISI 0.5 s, the mean aftereffect size was 0.79±0.31 °/s (mean ±SE). Panel **B**: ISI 1.0 s, 0.67±0.14 °/s. Panel **C**: ISI 1.5 s, 0.26±0.14 °/s. Panel **D**: ISI 3.0 s, 0.09±0.09 °/s.

"MATERIALS AND METHODS" and shown in Figure 2. In all the subjects, the difference in biases with adapter direction was in the direction consistent with an aftereffect for the 1 s adapter/test stimulus pairs for the short ISIs of 0.5 and 1.0 s (Fig. 4). With longer ISI, the aftereffect was generally smaller.

There was significant variation between subjects in both the detection threshold (Fig. 3B) and the size of the aftereffect (Fig. 4). A single subject (#5) had a very large aftereffect even though the threshold in this subject was not extreme.

A 1.5 s adapting stimulus with a displacement similar to the 1 s adapter was used with a 1.5 s test stimulus. These conditions were performed with NF and demonstrated a significant aftereffect in four of seven subjects (Fig. 5A). Interestingly, this condition sometimes produced a large aftereffect for some subjects (e.g., subject #9) who had only a minimal aftereffect with a 1 s test stimulus and adapter. There was a negative correlation between the size of the aftereffect with the 1 s adapter/test and the 1.5 s adapter/test (R=−0.32) although this trend was not significant (p=0.36).

Six of the nine subjects (2, 3, 4, 6, 7, 9) completed the NF portion experiment with slightly altered stimulus parameters. Using the same ISIs of 0.5, 1.0, 1.5, and 3 s, the adaptive stimulus was lengthened from 1.0 to 1.5 s (peak velocity 20 °/s), and the test stimulus was shortened from 1.0 to 0.5 s. The subjects showed no reliable aftereffect at the new adaptive and test stimulus frequencies, even though they did demonstrate considerable aftereffect in the protocols with the adapter and test stimuli with similar durations (individual data not shown).

The bias in the perception of the test stimulus caused by the adapter (aftereffect) was larger with shorter ISI (Fig. 6A) for both conditions with FP and NF. These conditions were only done with the 1 s adapter and 1 s test stimulus and were not repeated for the other stimulus conditions because they had no influence on the size of the aftereffect. However, the effect of ISI on the aftereffect size was significant when an adapting stimulus was given (ANOVA, p=0.002, F=5.21; Kruskal–Wallis, p<0.001, H=164). Similarly the threshold for discrimination of the test stimulus was significantly higher after shorter ISI (Fig. 5B, ANOVA, p=0.003, F=4.92; Kruskal–Wallis, p<0.001, H=78).

With increasing ISI, the aftereffect diminished and the threshold approached the baseline value. The decrease of both was closely approximated using an exponential decay function (Fig. 7). The time constant of the aftereffect decay was 1.05 s when fit to the data combined across all subjects (Fig. 7A) for a 1 s adapter and test stimulus. The time constant of the decay of the threshold to the baseline value was similar at 1.33 s when fit to the combined data (Fig. 7B). The aftereffect was only definitively present at a 0.5 s ISI with the 1.5 s adapter/test stimulus pair and could not be demonstrated with the 1.5 s adapter which was paired with a 0.5 s test stimulus (Fig. 7A). However, all of the conditions demonstrated a similar

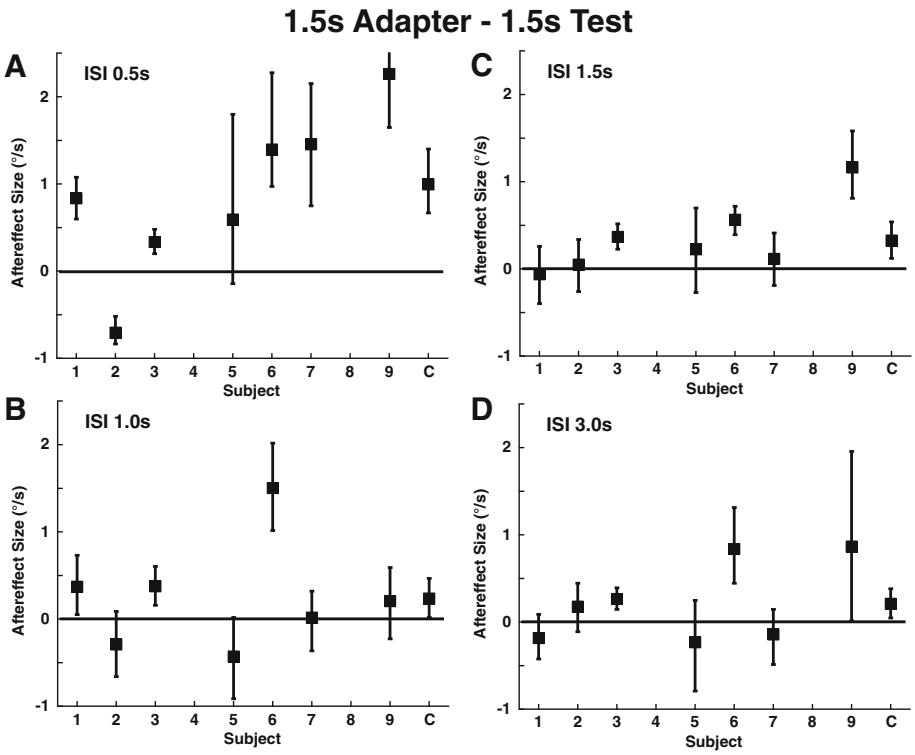

FIG. 5. Aftereffect size with a 1.5 s adapter and 1.5 s test stimulus. All were done with NF, using the previously described bootstrapping method. Error bars represent the 95 % confidence interval. Panel **A**: ISI 0.5 s, the mean aftereffect size was 0.88±0.36 °/s (mean±SE). Panel **B**: ISI 1.0 s, 0.25±0.24 °/s. Panel **C**: ISI 1.5 s, 0.34±0.16 °/s. Panel **D**: ISI 3.0 s, 0.23±0.18 °/s.

increase in threshold after an adapting stimulus even when no aftereffect was present (Fig. 7B).

An exponential decay function was also fit to the individual data which demonstrated a mean time constant of 1.2±0.6 (mean±SD) with a range of 0.6 to 2.5 s for a 1 s adapter and 1 s test stimulus (Table 1). However, in three subjects, the aftereffect size was poorly predicted by an exponential decay function as determined by the coefficient of determination for the best fit being below zero, indicating that simply using the average value at every time point fit better than the best fit of the function. This occurred in subjects 1 and 9 because there were negative aftereffects at some ISIs. In subject 6, there was an aftereffect which increased slightly at later ISIs. These subjects tended to have time constants at the extremes of the range, but when these three subjects were excluded from the average, the time constant remained essentially the same 1.2±0.4 s (range 0.7 to 1.9). This exponential decay function was also fit to individual subjects in the 1.5 s adapter/test stimulus condition and found to have a slightly shorter average time constant at 0.8±0.3 s (range 0.2 to 2.2).

To understand the current results in terms of velocity storage, a control systems model was implemented. The model implements the two main features of previous velocity storage models (Fig. 8): First, there is an element that implements the known dynamics of the semicircular canals with a time constant of about 4 s. In the current model, the canal time constant (τ_C) was set as 4 s. The second feature is also a central velocity storage loop (referred to in some previous models as the VSM) which has a time constant (τ_L) that is meant to correct the semicircular canal dynamics. In the proposed model, the loop time constant is also set to 4 s. The central velocity storage loop also has an output gain (G_o) and an internal gain (G_i). With just these elements, and both gains set to unity, the output of the system (perceived velocity) will exactly match the head velocity. However, real biological systems have noise and cannot operate this way because the noise would lead to large offsets over time which do not occur (Laurens and Angelaki 2011). For this reason, there is usually negative feedback built into the central velocity storage loop. To stimulate this, G_i is set to $-1/15$ s, a value previously found to fit vestibular perception after long duration rotation (Bertolini et al. 2011) and identified as a typical value in a recent review (Laurens and Angelaki 2011). However, this velocity storage model did not predict the current observations. Two additional models, both proposed to explain perceptual thresholds of low-frequency rotations, were closely examined and found to include only a semicircular canal with a time constant near 1 s and no velocity storage loop (Grabherr et al. 2008; Soyka et al. 2012). These models had a similar and much closer approximation of the current results (Fig. 8)

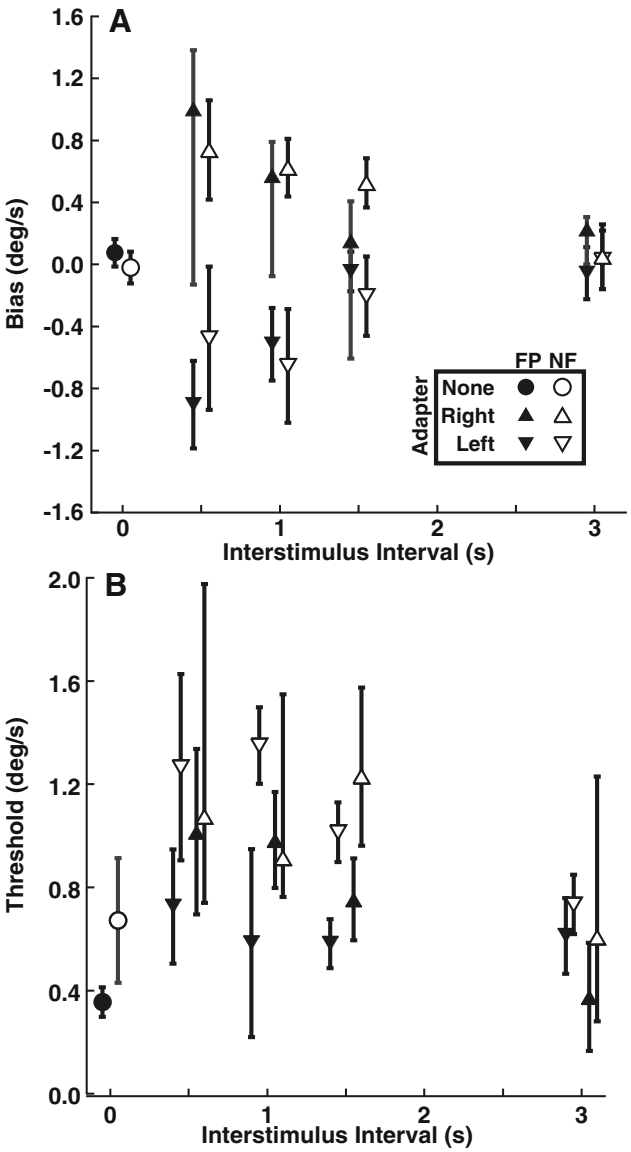

FIG. 6. The mean biases and thresholds for the study population by ISI for the 1 s adapter/test stimulus with both FP and NF conditions were tested. Error bars represent ±1 SEM. **A** Bias. **B** Threshold.

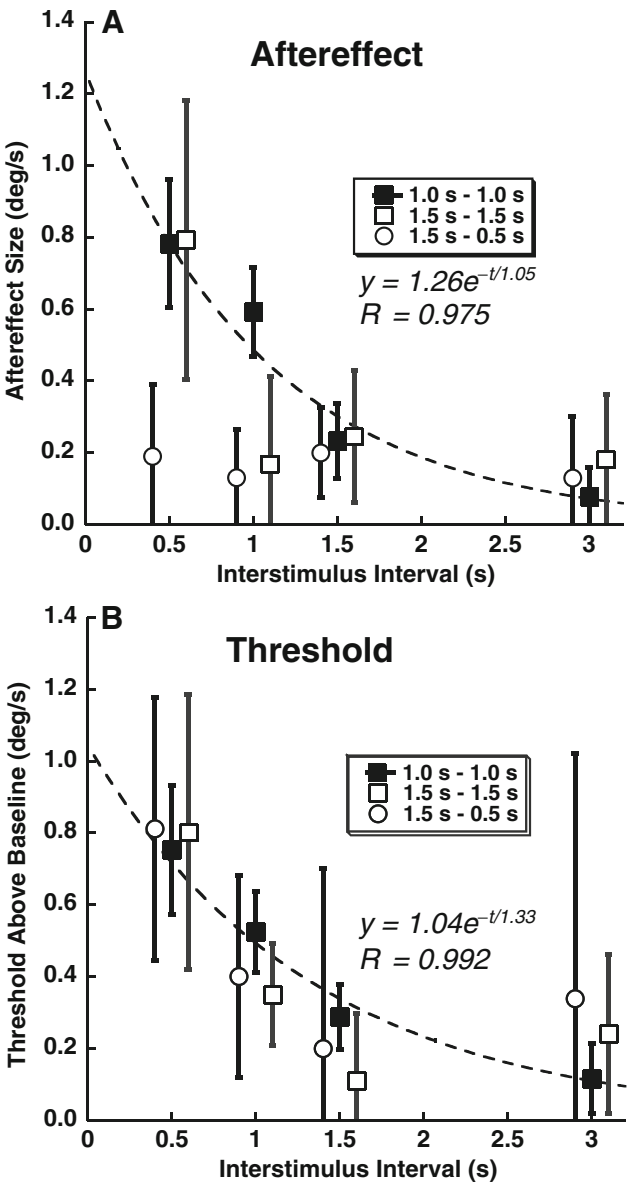

FIG. 7. Decay of aftereffect and increased threshold with time. The data are averaged across subjects and the FP/NF viewing conditions for the 1 s adapter/test (*filled squares*). For the 1.5 s adapter/test condition (*open squares*), the data represent the subjects who completed that study at only the NF viewing condition. The *open circles* represent the six subjects who completed the 1.5 s adapter, 0.5 s test stimulus condition. Error bars represent ±1 SEM. For clarity, the ISI on the 1.5 s adapter conditions have been displaced slightly, and curve fits represent only the 1 s–1 s condition which had better quality fits. **A** The aftereffect size as a function of ISI. **B** Threshold above baseline as a function of ISI. The baseline threshold was determined by presenting the test stimulus without an adapting stimulus (0.62 °/s) and subtracted from the threshold here. Thus, zero indicates the baseline threshold.

DISCUSSION

The current results demonstrate a perceptual aftereffect for yaw rotation. Despite variation between subjects in the size of the effect, most subjects demonstrated the phenomenon. To our knowledge, this is the first time such an aftereffect has been described in yaw. When considered in the context of other modes of sensory perception, this finding is not surprising. But in the context of previous studies of yaw rotation perception that have focused on long duration stimuli in which velocity storage is predominant (Keller and Henn 1984; Sinha et al. 2008; Bertolini et al. 2011; Bertolini et al. 2012), these findings may be unexpected. The reason aftereffects were not found in the previous studies was likely because the duration of stimuli was relatively long (i.e., on the order of minutes) a time course where velocity storage may be predominant.

TABLE 1

Fit of exponential decay function to individual aftereffect data by subject. Data from each subject were fit to the equation $y = Ce^{-t/\tau}$, where y is the size of the after effect, C is a constant which represents the predicted aftereffect at the end of the stimulus, and τ is the time constant. The coefficient of determination (R^2) was determined for each fit. In individuals marked with an asterisk, the calculated coefficient of determination was less than zero indicating that the average value fits the observations better than the best fit of the model. Boxes were left blank for some subjects with the 1.5 s – 1.5 s condition if the subject was no longer available for testing

	1	*2*	*3*	*4*	*5*	*6*	*7*	*8*	*9*
1 s – 1 s									
C (°/s)	0.52	0.40	1.06	0.89	5.46	1.13	1.64	0.72	0.01
τ (s)	0.60	1.42	1.12	1.93	0.97	0.62	0.71	2.48	1.05
R^2	*	0.40	0.79	0.69	0.96	*	0.97	0.22	*
1.5 s – 1.5 s									
C (°/s)	1.87	−2.11	−2.09		1.49	1.76	6.18		3.14
τ (s)	0.620	0.45	0.24		0.53	2.18	0.34		1.51
R^2	0.86	0.86	*		0.18	0.37	0.92		*

The current study was designed to identify the mean of a CDF rather than threshold (i.e., sigma or the width of the CDF). The staircase used (1-up, 1-down with variable step size) tended to concentrate most stimuli at the end of a trial block near the mean rather than at the shoulders of the psychometric

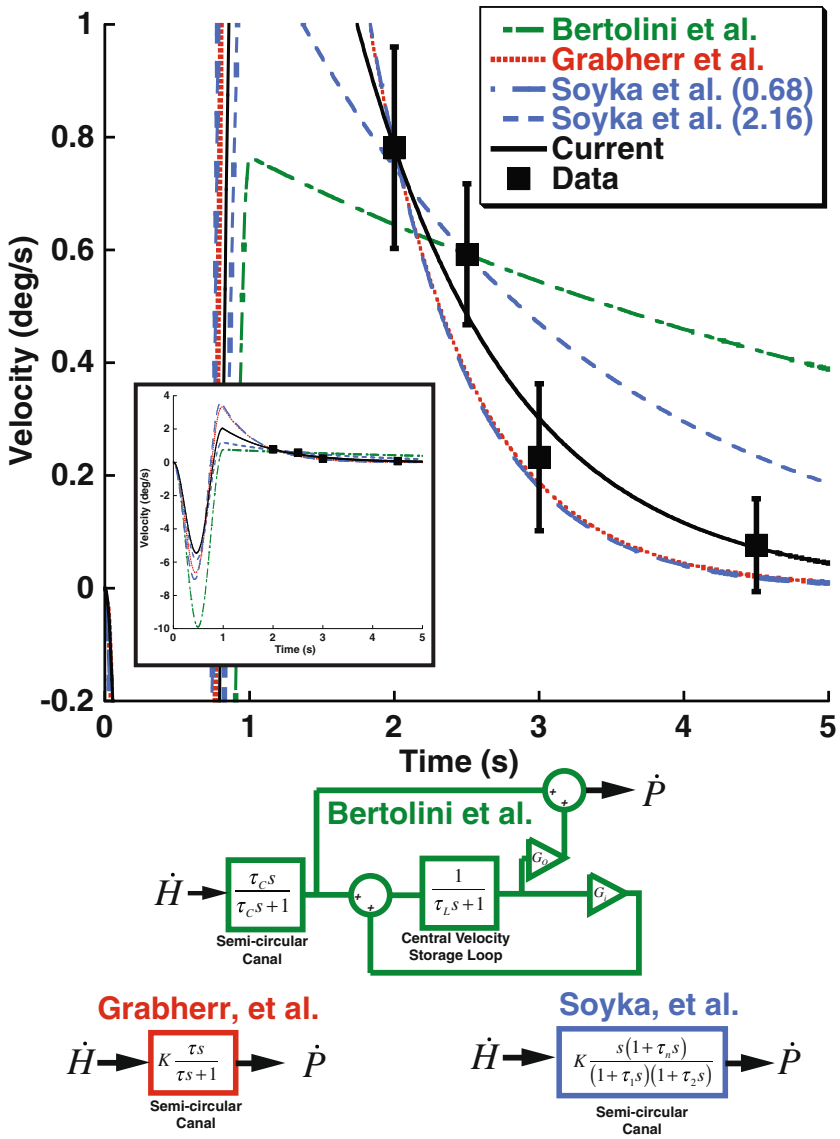

FIG. 8. Predictions of previous models of yaw rotation perception. Data points shown in Figure 7 for the 1 s adapter/test stimuli are included (*squares*) with error bars representing ±1 SEM to demonstrate the observed aftereffect size. Note that these points are plotted at the time their respective test stimulus would have reached its peak velocity rather than the ISI itself. The *inset* shows the full range of the models. In all models, s is the Laplace variable. The green model represents that proposed by Bertolini et al. based on the best fit to their data which was a canal time constant (τ_C) of 5.6 s, a VSM loop time constant (τ_L) of 15.5 s. The Bertolini et al. model also allows different gains of the input (G_i) and output (G_o) of the velocity storage loop. The red model was proposed by Grabherr et al. based on vestibular thresholds across a range of frequencies. It models the canals as a simple high-pass filter with a time constant (τ) of 0.7 s and does not include a VSM. The blue model proposed by Soyka et al. uses more parameters to describe the semicircular canals, but the dominant time constant (τ_1) was 0.68 s when fit to their data and 2.16 s when fit in a historical dataset. A constant (K) was varied to provide the best fit to the current data. The time constant in the Grabherr et al. model was allowed to vary and fit to the current data (black) which had a best time constant of 1.05 s. This is effectively the same fit performed in Figure 6.

function which might be better for determining threshold. Despite this, the results clearly demonstrated that the thresholds increased after an adapting stimulus, but the absolute values of these thresholds may not be accurate. This is especially true of extremely low thresholds as the minimum step size in the test stimulus was 0.4 °/s. Additionally, a recent paper has shown that adaptive psychometric techniques themselves can be a potential source of systematic errors when measuring threshold (Chaudhuri and Merfeld 2013). The thresholds reported here with the 1 Hz test stimulus alone and NF was identical to 0.9±0.7 °/s as previously reported in the current laboratory using a different staircase technique (Roditi and Crane 2012b) and similar to that found by others (Benson and Brown 1989; Grabherr et al. 2008). The current study controlled for factors that may have introduced systematic errors in the determination of the mean of the CDF by doing a control condition in which the test stimulus was presented without an adapter and by interleaving trials with adapting stimuli in opposite directions.

The recent literature on yaw rotation perception presents two competing models to describe perception. One model is based on perceived rotation after a long constant velocity rotation ends (Bertolini et al. 2011). This model predicts a prominent roll for the VSM with a time constant of 15.5 s, while the canal has a time constant of about 5.6 s (Fig. 8, green). The other model is based on perceptual thresholds of rotations at 0.2 Hz and below (Grabherr et al. 2008; Soyka et al. 2012). These similar threshold models propose a shorter canal time constant (~1 s) with no VSM component (Fig. 8, red and blue). The implications of both models with respect to the current findings will be considered in turn.

Applying the previously proposed model of rotation perception after a velocity step (Bertolini et al. 2011) to the current stimulus predicted an aftereffect with a decay time much longer than is observed (Fig. 8, green). Although the parameters for the model presented are based on the average of all their subjects, they divided subjects into three categories. However, all of these categories included relatively long time constants for the VSM and semicircular canals and hence did not provide a good fit of the current data. If the parameters of the model were varied individually, the model would fit better if the VSM was turned off due to the decrease of the time constant to that of the canals. However, that would still be too long to describe the current results. It should be mentioned that similar longer duration constant findings have also been reported by others in response to velocity steps (Keller and Henn 1984; Sinha et al. 2008). The reason this model does not fit is that both branches of the model (the semicircular canal and VSM) have time constants much longer than what is currently observed. Therefore, this model does not describe the response to relatively high-frequency stimuli such as those currently tested.

The other type of model includes only a semicircular canal and no central VSM (Fig. 8, red and blue). When thresholds of individual stimulus presentations were examined (Grabherr et al. 2008; Soyka et al. 2012), a sharp increase in thresholds at frequencies below 0.2 Hz has been described. This finding is consistent with a short semicircular canal time constant with no VSM. The time constant was estimated by Grabherr et al. to be 0.7 s. Soyka et al. estimated the time constant from their data using a slightly different model to be very similar 0.68 s, but when they included historical data sets (Benson et al. 1989), they found the time constant could be as long as 2.16 s. Thus, the thresholds were best described not only by the absence of velocity storage, but by a time constant significantly shorter than the previous ~4 s estimates of the human semicircular canal itself (Dai et al. 1999) based on measurements of the VOR or the 5.6 s estimated from perception after velocity steps (Bertolini et al. 2011). However, both of these studies predicted that the influence of this time constant on yaw rotation perceptual thresholds would be negligible above 0.5 Hz and did not consider the potential influence of a preceding stimulus such as that used in the current study. Despite the differences in the stimulus and task used, these models developed for perceptual thresholds of low-frequency rotations provided an excellent fit to the current data (Fig. 8). One of these models considered the semicircular canal as a simple first-order high-pass filter (Grabherr et al. 2008) while the other considered a model with more parameters although the models were fit using the same number of free parameters (Soyka et al. 2012). Both of these models found the dominant time constant to be similar at τ=0.7 s (Grabherr et al. 2008) or τ_1=0.68 s (Soyka et al. 2012). The predictions of these two models are virtually indistinguishable in the frequency domain tested in the current experiment (Fig. 8). Although all of these models provide a reasonable approximation of the current results (Fig. 8), the best fit to the data was with a time constant of 1.05 s using the simpler Grabherr et al. model. The aftereffects observed with the current stimulus parameters are consistent with a relatively short time constant of the canals with no influence on the VSM.

Velocity storage is classically studied during long-duration stimuli; thus, it is possible that the 1 and 1.5 s stimuli used here do not cause significant activation of this system. The control system model of velocity

storage (Fig. 8) proposed by others (Bertolini et al. 2011) does predict an effect for the stimulus used here, although this model was developed based on velocity step stimuli. Therefore, it is perhaps not surprising that it cannot be extrapolated to the much shorter stimuli presently studied. It has also been argued that velocity storage may function to overcome physical limitations of the semicircular canals which could help maintain rotation signals during 1–3 s rotations that occur during normal activity (MacNeilage et al. 2008; Laurens and Angelaki 2011). If this occurs, it is likely that the velocity storage system only influences reflex pathways in this time domain. In the current data, the presence of a fixation point had no influence on the time constant, even though such a visual stimulus greatly shortens the time constant of velocity storage (Cohen et al. 1977; Waespe and Schwarz 1986; Gizzi and Harper 2003). This study provides mounting evidence that the mechanisms of vestibular perception and vestibular reflexes are fundamentally different (Barnett-Cowan et al. 2005; Merfeld et al. 2005a, b; Bertolini et al. 2011).

The time constant of the rotational aftereffect reported here was about 1 s (Fig. 7). This is shorter than the previous reports of 4 s or longer estimated by others (Goldberg and Fernandez 1971; Dai et al. 1999; Ifediba et al. 2007; Bertolini et al. 2011), although the time constant of the human semicircular canal has not been directly measured. Two prior studies estimated the time constant to be ~1 s which is similar to the current study (Grabherr et al. 2008; Soyka et al. 2012). The time constant has also been estimated to be as short as 2 s in patients with congenital nystagmus (Demer and Zee 1984; Okada et al. 1999), and time constants near 1 s have been reported in monkeys after chronic electrical vestibular stimulation (Merfeld et al. 2007). The estimate of the semicircular canal time constant may depend on some degree on how it is measured. For instance, when VOR thresholds are used, the thresholds do not increase at 0.2 Hz suggesting a longer time constant (Haburcakova et al. 2012) than is suggested by similar perceptual threshold experiments (Soyka et al. 2012).

The current experiment demonstrated that yaw aftereffects were strongest when the test stimulus was the same duration as the adapter. The effect could be demonstrated using both 1 and 1.5 s stimulus adapter pairs. However, using a longer adapter (1.5 s) and shorter test stimulus (0.5 s) did not yield an aftereffect (Fig. 7), even though similar stimulus parameters have been demonstrated to produce perceptual aftereffects with fore-aft translation (Crane 2012b) and with roll (Crane 2012a). Large differences in the duration of the adapting and test stimuli have also been shown to induce aftereffects in several other sensory stimuli including visual (Hershenson 1993; Leopold et al. 2005; Bao and Engel 2012) and auditory motion (Neelon and Jenison 2004). A general theme in sensory aftereffects is that a longer period of adaptation leads to a stronger and longer aftereffect (Taylor 1963; Greenlee et al. 1991; Anstis et al. 1998; Neelon and Jenison 2004), but the current data presents a rare exception to this, at least when the test stimulus and adapter are different durations. This provides yet another reason why aftereffects may not have been observed after long duration adapting stimuli (Keller and Henn 1984; Sinha et al. 2008; Bertolini et al. 2011; Bertolini et al. 2012)—a similar duration test stimulus was not given.

In some subjects, the aftereffect was much stronger when the 1 s stimulus/adapter pair was used and all but absent for the 1.5 s stimulus adapter pair. The reverse was true in other subjects. The reason for this may be that the aftereffect is tuned to a frequency of yaw rotation commonly experienced during ambulation of about 1 Hz (Crane and Demer 1997) although the exact frequency likely varies between individuals which might explain the predominant frequency of the aftereffect. Since the type and frequency of motion during natural activities such as ambulation was not measured in these subjects, it will be left to future studies to investigate further.

In the current study, the mean aftereffect size was modest. At its strongest effect (0.5 s ISI and 1 s adapting/test stimulus), it still averaged about 0.8 °/s at 0.5 s or about 3 % of the size of the adapting stimulus. In a prior study in the current laboratory, after a smaller roll stimulus with a similar peak velocity at 12 °/s, the aftereffect amplitude was 3 °/s or about 25 % of the adapting stimulus (Crane 2012a). With a fore-aft translation adapter at 20 cm/s, the aftereffect was largest with a 1 s ISI due to a priming effect which was present in some subjects at 0.5 s. However at 1 s, the aftereffect was about 1.5 cm/s or about 8 % of the size of the adapting stimulus (Crane 2012b). With visual stimuli, the aftereffect was previously shown to be 60 % of the adapting stimulus (Crane 2013). The currently observed yaw aftereffect was comparatively but a fraction of the adapting stimulus. Also, the 1.5 s adapter followed by a 0.5 s test stimulus that was previously used for roll and fore-aft translation did not yield any aftereffect in the current study (Fig. 7).

Given that derangements in velocity storage have been implicated as a mechanism of human pathology (Dai et al. 2003; Bertolini et al. 2012), it is also possible that derangements in vestibular aftereffects could also give risk to clinically significant pathology such as motion sickness or motion intolerance.

The frequencies of stimulation studied here (1 and 0.66 Hz) are highly relevant and near the predominant frequency of yaw rotation during human ambu-

lation (Grossman et al. 1989; Crane and Demer 1997). The adapting stimulus used here was larger (12 °) than is typical during ambulation (2–3 °) (Crane and Demer 1997), but the test stimulus at the point at which subjects are equally likely to perceive rightward vs. leftward rotation is smaller. The current stimulus conditions are also different from ambulation in that the stimuli were limited to a single frequency and there were not simultaneous stimuli in other directions. The current data demonstrates that perception of repeating stimuli at the same frequency is such that the perceptual bias and threshold of subsequent stimuli make them less likely to be perceived. Therefore, these rotational aftereffects may act as a filter allowing only the most atypical and potentially salient vestibular stimuli to be perceived.

ACKNOWLEDGMENTS

This work was funded by a grant from the NIDCD (K23 DC011298) with additional support provided by a clinician-scientist grant from the Triological Society. Technical support was provided by Shawn Olmstead-Leahey.

Conflict of Interest The authors declare no competing financial interests.

REFERENCES

ADDAMS R (1834) An account of a peculiar optical phaenomenon seen after having looked at a moving body etc. Mag J Sci 3rd Ser 5:373–374

ANSTIS S, VERSTRATEN FA, MATHER G (1998) The motion aftereffect. Trends Cogn Sci 2:111–117

BAO M, ENGEL SA (2012) Distinct mechanism for long-term contrast adaptation. Proc Natl Acad Sci U S A 109:5898–5903

BARNETT-COWAN M, DYDE RT, HARRIS LR (2005) Is an internal model of head orientation necessary for oculomotor control? Ann N Y Acad Sci 1039:314–324

BENSON AJ, BROWN SF (1989) Visual display lowers detection threshold of angular, but not linear, whole-body motion stimuli. Aviat Space Environ Med 60:629–633

BENSON AJ, SPENCER MB, STOTT JR (1986) Thresholds for the detection of the direction of whole-body, linear movement in the horizontal plane. Aviat Space Environ Med 57:1088–1096

BENSON AJ, HUTT EC, BROWN SF (1989) Thresholds for the perception of whole body angular movement about a vertical axis. Aviat Space Environ Med 60:205–213

BERTOLINI G, RAMAT S, LAURENS J, BOCKISCH CJ, MARTI S, STRAUMANN D, PALLA A (2011) Velocity storage contribution to vestibular self-motion perception in healthy human subjects. J Neurophysiol 105:209–223

BERTOLINI G, RAMAT S, BOCKISCH CJ, MARTI S, STRAUMANN D, PALLA A (2012) Is vestibular self-motion perception controlled by the velocity storage? Insights from patients with chronic degeneration of the vestibulo-cerebellum. PLoS One 7:e36763

BESTELMEYER PE, ROUGER J, DEBRUINE LM, BELIN P (2010) Auditory adaptation in vocal affect perception. Cognition 117:217–223

CHAUDHURI SE, MERFELD DM (2013) Signal detection theory and vestibular perception: III. Estimating unbiased fit parameters for psychometric functions. Exp Brain Res 225:133–146

COHEN B, MATSUO V, RAPHAN T (1977) Quantitative analysis of the velocity characteristics of optokinetic nystagmus and optokinetic after-nystagmus. J Physiol 270:321–344

COHEN B, HENN V, RAPHAN T, DENNETT D (1981) Velocity storage, nystagmus, and visual-vestibular interactions in humans. Ann N Y Acad Sci 374:421–433

CRANE BT (2012A) Roll aftereffects: influence of tilt and inter-stimulus interval. Exp Brain Res 233:89–98

CRANE BT (2012B) Fore-aft translation aftereffects. Exp Brain Res 219:477–487

CRANE BT (2013) Limited interaction between translation and visual motion aftereffects in humans. Exp Brain Res 224:165–178

CRANE BT, DEMER JL (1997) Human gaze stabilization during natural activities: translation, rotation, magnification, and target distance effects. J Neurophysiol 78:2129–2144

DAI M, KLEIN A, COHEN B, RAPHAN T (1999) Model-based study of the human cupular time constant. J Vestib Res 9:293–301

DAI M, KUNIN M, RAPHAN T, COHEN B (2003) The relation of motion sickness to the spatial-temporal properties of velocity storage. Exp Brain Res 151:173–189

DEMER JL, ZEE DS (1984) Vestibulo-ocular and optokinetic deficits in albinos with congenital nystagmus. Investig Ophthalmol Vis Sci 25:739–745

ERCOLINE WR, DEVILBISS CA, YAUCH DW, BROWN DL (2000) Post-roll effects on attitude perception: "the Gillingham Illusion". Aviat Space Environ Med 71:489–495

FETSCH CR, TURNER AH, DEANGELIS GC, ANGELAKI DE (2009) Dynamic re-weighting of visual and vestibular cues during self-motion perception. J Neurosci 29:15601–15612

GIZZI MS, HARPER HW (2003) Suppression of the human vestibulo-ocular reflex by visual fixation or forced convergence in the dark, with a model interpretation. Curr Eye Res 26:281–290

GOLDBERG JM, FERNANDEZ C (1971) Physiology of peripheral neurons innervating semicircular canals of the squirrel monkey. I. Resting discharge and response to constant angular accelerations. J Neurophysiol 34:635–660

GRABHERR L, NICOUCAR K, MAST FW, MERFELD DM (2008) Vestibular thresholds for yaw rotation about an earth-vertical axis as a function of frequency. Exp Brain Res 186:677–681

GREENLEE MW, GEORGESON MA, MAGNUSSEN S, HARRIS JP (1991) The time course of adaptation to spatial contrast. Vis Res 31:223–236

GROSSMAN GE, LEIGH RJ, BRUCE EN, HUEBNER WP, LANSKA DJ (1989) Performance of the human vestibuloocular reflex during locomotion. J Neurophysiol 62:264–272

HABURCAKOVA C, LEWIS RF, MERFELD DM (2012) Frequency dependence of vestibuloocular reflex thresholds. J Neurophysiol 107:973–983

HERSHENSON M (1993) Linear and rotation motion aftereffects as a function of inspection duration. Vis Res 33:1913–1919

IFEDIBA MA, RAJGURU SM, HULLAR TE, RABBITT RD (2007) The role of 3-canal biomechanics in angular motion transduction by the human vestibular labyrinth. Ann Biomed Eng 35:1247–1263

KELLER G, HENN V (1984) Self-motion sensation influenced by visual fixation. Percept Psychophys 35:279–285

LAURENS J, ANGELAKI DE (2011) The functional significance of velocity storage and its dependence on gravity. Exp Brain Res Exp Hirnforsch Exp Cereb 210:407–422

LEOPOLD DA, RHODES G, MULLER KM, JEFFERY L (2005) The dynamics of visual adaptation to faces. Proc Biol Sci R Soc 272:897–904

MACNEILAGE PR, GANESAN N, ANGELAKI DE (2008) Computational approaches to spatial orientation: from transfer functions to dynamic Bayesian inference. J Neurophysiol 100:2981–2996

MacNeilage PR, Banks MS, DeAngelis GC, Angelaki DE (2010) Vestibular heading discrimination and sensitivity to linear acceleration in head and world coordinates. J Neurosci 30:9084–9094

Mather G, Pavan A, Campana G, Casco C (2008) The motion aftereffect reloaded. Trends Cogn Sci 12:481–487

Merfeld DM, Park S, Gianna-Poulin C, Black FO, Wood S (2005a) Vestibular perception and action employ qualitatively different mechanisms. I. Frequency response of VOR and perceptual responses during Translation and Tilt. J Neurophysiol 94:186–198

Merfeld DM, Park S, Gianna-Poulin C, Black FO, Wood S (2005b) Vestibular perception and action employ qualitatively different mechanisms. II. VOR and perceptual responses during combined Tilt&Translation. J Neurophysiol 94:199–205

Merfeld DM, Haburcakova C, Gong W, Lewis RF (2007) Chronic vestibulo-ocular reflexes evoked by a vestibular prosthesis. IEEE Trans Biomed Eng 54:1005–1015

Neelon MF, Jenison RL (2004) The temporal growth and decay of the auditory motion aftereffect. J Acoust Soc Am 115:3112–3123

Nooij SA, Groen EL (2011) Rolling into spatial disorientation: simulator demonstration of the post-roll (Gillingham) illusion. Aviat Space Environ Med 82:505–512

Okada T, Grunfeld E, Shallo-Hoffmann J, Bronstein AM (1999) Vestibular perception of angular velocity in normal subjects and in patients with congenital nystagmus. Brain 122(Pt 7):1293–1303

Raphan T, Matsuo V, Cohen B (1979) Velocity storage in the vestibulo-ocular reflex arc (VOR). Exp Brain Res Exp Hirnforsch Exp Cereb 35:229–248

Reinhardt-Rutland AH (1990) Note on aftereffect of unidirectional sound-level change with different durations of test stimulus. Percept Mot Skills 70:635–638

Robinson DA (1977) Linear addition of optokinetic and vestibular signals in the vestibular nucleus. Exp Brain Res 30:447–450

Roditi RE, Crane BT (2012a) Suprathreshold asymmetries in human motion perception. Exp Brain Res 219:369–379

Roditi RE, Crane BT (2012b) Directional asymmetries and age effects in human self-motion perception. J Assoc Res Otolaryngol 13:381–401

Seizova-Cajic T, Smith JL, Taylor JL, Gandevia SC (2007) Proprioceptive movement illusions due to prolonged stimulation: reversals and aftereffects. PLoS One 2:e1037

Sinha N, Zaher N, Shaikh AG, Lasker AG, Zee DS, Tarnutzer AA (2008) Perception of self motion during and after passive rotation of the body around an earth-vertical axis. Prog Brain Res 171:277–281

Soyka F, Giordano PR, Barnett-Cowan M, Bulthoff HH (2012) Modeling direction discrimination thresholds for yaw rotations around an earth-vertical axis for arbitrary motion profiles. Exp Brain Res 220:89–99

Taylor MM (1963) Tracking the decay of the after-effect of seen rotary movement. Percept Mot skills 16:119–129

Thompson P, Burr D (2009) Visual aftereffects. Curr Biol: CB 19:R11–R14

Valko Y, Lewis RF, Priesol AJ, Merfeld DM (2012) Vestibular labyrinth contributions to human whole-body motion discrimination. J Neurosci 32:13537–13542

Waespe W, Schwarz U (1986) Characteristics of eye velocity storage during periods of suppression and reversal of eye velocity in monkeys. Exp Brain Res 65:49–58

Wichmann FA, Hill NJ (2001a) The psychometric function: I. Fitting, sampling, and goodness of fit. Percept Psychophys 63:1293–1313

Wichmann FA, Hill NJ (2001b) The psychometric function: II. Bootstrap-based confidence intervals and sampling. Percept Psychophys 63:1314–1329

Young LR, Oman CM (1969) Model for vestibular adaptation to horizontal rotation. Aerosp Med 40:1076–1080